Journal Name

RSCPublishing

ARTICLE

# Crystal growth of MOF-5 using secondary building units studied by *in situ* atomic force microscopy

Cite this: DOI: 10.1039/xoxxoooooox

Pablo Cubillas,[a#] Kimberley Etherington,[a] Michael W. Anderson,[a] and Martin P. Attfield[a*]

Received ooth January 2012,
Accepted ooth January 2012

DOI: 10.1039/xoxxoooooox

www.rsc.org/

Crystal growth of the metal-organic framework, MOF-5, using basic zinc benzoate, $[Zn_4O(O_2CC_6H_5)_6]$, was studied in real time using atomic force microscopy. The two-dimensional nuclei involved in layer growth were found to form by a two-step process whereby 1,4-benzenedicarboxylate units first attach to the MOF-5 surface followed by addition of a layer of Zn species and connecting 1,4-benzenedicarboxylate units. No evidence of a growth mechanism involving nucleophilic substitution of a benzoate group from an intact $[Zn_4O(O_2CC_6H_5)_6]$ molecule by a surface attached 1,4-benzenedicarboxylate unit was found. This indicates that the $[Zn_4O(O_2CC_6H_5)_6]$ molecules undergo a degree of dissociation before incorporation into the MOF-5 framework. The $[Zn_4O(O_2CC_6H_5)_6]$-containing growth solutions were found to influence the relative growth rates along different crystallographic directions and to lead to a faster nucleation rate under certain conditions when compared to growth solutions containing simpler zinc salts. This suggests a degree of remnant association of the zinc species derived from the $[Zn_4O(O_2CC_6H_5)_6]$ cluster during crystal growth under these conditions.

## Introduction

Porous metal-organic frameworks (MOFs) are formed from the connection of metal ions and organic linkers to provide an enormous number of different structures of varying pore dimension, geometry and functionality that are finding potential use in a diverse array of new and traditional applications.[1-4] Considerable effort has been expended to optimise the synthesis of these materials with regards to numerous factors including: yield, crystal size, morphological control, the rate of product formation and the synthesis temperature. One such approach to the synthesis of MOFs is the so called "controlled secondary building unit (SBU) approach" (CSA) introduced by Serre *et al.*[5] The rationale behind the development of this approach was that MOF syntheses could be speeded up if the metal components added to the reaction solution were already pre-assembled to resemble the SBUs of the final crystalline MOF. This method has succeeded in decreasing reaction times and temperatures for several MOFs,[5-7] in addition to proving to be very useful in the synthesis of nanoparticles,[8] thin films,[9] and producing MOF homologues with new metal content.[6]

One of the questions arising from the CSA methodology is whether the SBU remains intact during synthesis. If it does then this would suggest that formation of the MOF can occur via a simple ligand substitution reaction of the non-bridging ligands attached to the SBU for the bridging organic linkers found in the resulting MOF. There is currently a paucity of information on this issue. A pseudo *in situ* EXAFS investigation of the formation of MIL-89, $[Fe_3O(CH_3OH)_3(muc)_3]Cl\cdot(CH_3OH)_6$, (muc = *trans–trans*-muconate) provided some evidence for the presence of the trimeric ferric acetate SBU throughout the formation of the MOF using a highly restrained structural model to fit the experimental data collected from a reaction solution cooled to room temperature after the onset of crystallisation of the MIL-89 product.[10] Some spectroscopic evidence for the retention of the SBU structure of basic zinc perfluoromethylbenzoate after the initial deposition onto the carboxylate group of a 16-mercaptohexadecanoic acid self-assembled monolayer has also been reported,[9] although subsequent formation of MOF-5 using this SBU was not pursued.

Atomic force microscopy (AFM) has proven itself to be one of the most useful techniques in deciphering the crystal growth process of crystallisation due to its ability to scan surface features with a vertical resolution < 0.1 nm and the capacity to perform *in situ* studies.[11-14] *In situ* AFM studies of differing resolution have been reported for a number of MOFs,[15-19] revealing valuable information concerning their crystal growth and the growth of nanoporous materials.

MOF-5 $[Zn_4O(bdc)_3]$ (bdc = 1,4-benzenedicarboxylate) is one of the archetypal permanently porous MOFs[20] that consists of $(Zn_4O)^{6+}$ units connected by $bdc^{2-}$ linkers to form a cubic

network (space group *Fm-3m*) as shown in Fig. 1. The orientation of the carboxylate linkers alternate along each unit cell axis resulting in a unit cell length of $a$ = 25.669 Å. MOF-5 has successfully been synthesised with the CSA approach using basic zinc acetate or basic zinc benzoate $[Zn_4O(O_2CC_6H_5)_6]$ as SBUs and with products forming in minutes from syntheses performed in the temperature range 25 – 100 °C.[6]

In this work, *in situ* AFM was used to observe, for the first time, the crystal growth of MOF-5 using a CSA method with the aim of establishing the influence of a SBU on the growth mechanism, the morphology of growing terraces and the surface nucleation and terrace spreading rates when compared to MOF-5 surface growth using conventional growth solutions prepared using zinc nitrate or zinc acetate salts.[19]

## Experimental

The MOF-5 seed crystals used in the AFM experiments were synthesised on glass cover slides following the procedure of Rowsell.[21] $Zn(NO_3)\cdot 4H_2O$ (Merck) was mixed in solid form with $H_2$bdc (SigmaAldrich), and then *N,N'*-diethylformamide (DEF) (TCI) was added as the solvent. The molar composition of the synthesis solution was: 1 Zn: 0.33 $H_2$bdc: 111 DEF. Glass cover slides were introduced in the vial containing the reagent solution. The vial was then sealed and placed in an oven at 90 °C for 48 hours. *In situ* growth experiments were performed by introducing the seed crystal covered slide in a temperature-controlled open fluid cell (Biocell, JPK Instruments AG) which was then attached to the AFM (Nanowizard II, JPK Instruments AG). Only crystals with facets approximately parallel to the glass slide surface were scanned to minimize artefacts derived from the non-linearity of the piezo displacement on the *z*-axis. The crystals were kept in the mother solution all the time prior to introduction of the growth solutions. Growth solutions were always exchanged three times prior to the onset of imaging to prevent any dilution effects and contamination from the previous solutions. Powder X-ray diffraction (PXRD) confirmed the formation of the substrate crystals as MOF-5 as shown in Electronic Supplementary Information (ESI) Fig. ESI1 and scanning electron microscopy revealed the expected cubic morphology of the MOF-5 crystals as shown in Fig. ESI2.

The basic zinc benzoate SBU precursor $[Zn_4O(O_2CC_6H_5)_6]$ was prepared following a two-step synthesis, using procedures by Blustein[22] and Clegg.[23] In the first step, a binary zinc benzoate $[Zn(O_2CC_6H_5)_2]$ was prepared by adding, drop-wise, a 0.33 M $Zn(NO_3)\cdot 6H_2O$ (AlfaAesar) solution (9.817 g in 100 mL water) into a beaker containing 1 M ammonium benzoate solution (13.915 g in 100 mL water), under continuous stirring. Once the addition of the zinc nitrate solution was complete, the solution was stirred for 1 hour. The precipitate was filtered off and washed three times with a $10^{-3}$ M ammonium benzoate solution (0.0139 g in 100 mL water) to avoid hydration of the precipitate, and dried. In the second step, 0.5 g of the $[Zn(O_2CC_6H_5)_2]$ was dissolved in a minimum quantity of acetone (~130 mL) (Sigma Aldrich, <0.1% water content) under gentle heating. The resulting solution was filtered while hot and then cooled to < 0 °C. Crystals formed over a period of few days at this < 0 °C temperature.[6, 23] PXRD confirmed the formation of the basic zinc benzoate SBU precursor $[Zn_4O(O_2CC_6H_5)_6]$ as shown in Fig. ESI3.

The growth solutions used in the *in situ* AFM experiments are listed in Table 1 along with details on the naming scheme for each solution. Typical examples of solution preparations are as follows: an **α1** solution was made by adding a solution of $Zn(CH_3COO)_2\cdot 2H_2O$ (Sigma) in *N,N'*-dimethylformamide (DMF) (AlfaAesar) was to a solution of $H_2$bdc (SigmaAldrich) and triethlyamine (TEA) (Fluka) in DMF; a **β1** solution was made by adding a solution of $[Zn_4O(O_2CC_6H_5)_6]$ in DMF to a solution of $H_2$bdc in DMF; a **γ1** solution was made by adding a solution of $Zn(CH_3COO)_2\cdot 2H_2O$ in DMF to a solution of $H_2$bdc in DMF; a **β2** solution was made by adding a solution of $[Zn_4O(O_2CC_6H_5)_6]$ in acetone to a solution of $H_2$bdc predissolved in a minimum amount of DMF. The acetone/ DMF ratio was 40:1 in the resulting **β2** solutions.

All *in situ* growth AFM experiments were conducted in contact mode using silicon rectangular-shaped cantilevers with a radius of curvature of the tip less than 10 nm, and a force constant of 0.15 N $m^{-1}$ (CSC17/no Al supplied by MikroMasch). All experiments were carried out at loads close to zero nN, as it was found that increasing the load above 5 nN severely influenced the experiment, either by arresting the growth or by inducing dissolution through etch pit formation. In all experiments zoomed-out scans were performed around previously scanned areas to verify that the load did not have any effect on the observed results. No effect of prior scanning was observed on these areas in all experiments reported hereinafter.

Image analysis was carried out using the JPK Image Processing software (JPK Instruments AG). Height images were flattened by first applying a first order line by line fit and then a plane fit to further correct for any tilt. Deflection images were left untreated. Height analysis of step heights was carried out in about a dozen images using the histogram tool to sample a larger area around the step. Height analysis of 2D nuclei was only performed by cross section analysis due to the limited sized of the nuclei. Terrace spreading rates were determined by either measuring the half-length of a spreading terrace produced from a 2-D nuclei along the <100> directions (or <110> for experiments with $Zn/H_2$bdc ≈1) or by using a screw dislocation as a reference point from which to measure distances. Measurements were done over a time span of 15 - 30 minutes utilizing the first 8 - 15 images recorded after injection of a new growth solution thus minimizing any effect of decreasing supersaturation due to nutrient depletion. Nucleation rates per unit area were calculated from plots of the number of nuclei formed per unit area against time. The first four frames taken after introduction of a new solution were used to obtain the values of the nucleation rates per unit area. The number of nuclei per unit surface area was counted from the first scan taken after solution injection in experiments where the change in nucleation rate was too fast to measure it directly (i.e. only an initial "burst" of nuclei was observed). The latter

 

measurements provided a comparator to compare the nucleation behaviour for certain sets of growth solutions.

PXRD patterns were obtained using a Philips X'pert diffractometer. Representative samples were ground prior to mounting on the sample holder. Data were collected in the 2θ range of 3 - 60° using Cu-$K_\alpha$ radiation, with a wavelength of 1.54 Å. Scanning electron micrographs were taken using a Quanta environmental electron microscope.

## Results and discussion

All the *in situ* crystal growth experiments (**A** – **E**) involving very dilute growth solutions (see Table 1 for details) resulted in new crystal growth of MOF-5 on the crystal surface of the substrate crystals as determined from the consistently determined step height value of 1.3 ± 0.1 nm on the expressed crystal facet. This height corresponds to the $d_{200}$-spacing as reported in previous work.[19] Results from one such experiment, **A**, using DMF as the solvent are shown in Fig. 2. The experiment was started by introducing a growth solution (**SA1-α1-21**) to initiate the new growth of MOF-5 on the surface of the substrate crystals. Growth occurred via an initial burst of 2-D nucleation, followed by growth through step advancement. The **SA1-α1-21** solution was left in the cell for approximately 2 hours during which the step advancement rate decreased noticeably. At this point a new growth solution, **SA2-β1-4**, containing the basic zinc benzoate SBU $[Zn_4O(O_2CC_6H_5)_6]$ was introduced into the fluid cell. The new solution promoted 2-D nucleation immediately, as can be seen in the AFM deflection image show in Fig. 2a, taken 4 minutes after solution injection. Only a few nuclei were observed to form in subsequent images, and after 10 minutes all nucleation stopped. The growth of MOF-5 using $[Zn_4O(O_2CC_6H_5)_6]$ followed a similar pattern to that observed previously.[19] The shape of the nuclei and terraces formed was almost perfectly square with edges parallel to the <100> direction, again following the same trends observed for MOF-5 grown from the **α1**-type solutions.[19] The step advancement speed was approximately 0.021 ± 0.005 nm $s^{-1}$ measured during the 20 minute period after solution injection. Height analysis of the first nuclei formed from the $[Zn_4O(O_2CC_6H_5)_6]$-containing **SA2-β1-4** solution on the MOF-5 crystal surface grown from solution **SA1-α1-21** was performed and revealed a minimum height of approximately 0.8 ± 0.1 nm, as can be seen in the representative measurement shown in Fig. 2a for the nucleus highlighted in the white circle. The same nuclei was measured in the subsequent image collected 2 minutes later, that revealed a height of approximately 1.3 ± 0.1 nm, see Fig. 2b. This sequence of heights was measured from more than 10 similarly developing nuclei growing on MOF-5 surfaces previously grown from a **α1**-type solution across various experiments, but in no case were values larger than 1.3 nm ever observed. These two height values correspond to the attachment of a $bdc^{2-}$/ $Hbdc^-$ species on the MOF-5 surface (Fig. 2a) followed by subsequent growth of the of $Zn_4O$ cluster plus cross-linking $bdc^{2-}$ species parallel to the surface to complete the stable extended step corresponding to half the unit cell of the MOF-5 structure. This nucleation behaviour follows that which has been reported before for growth solutions prepared using zinc nitrate or zinc acetate salts.[18, 19]

An experiment (**E** – see Table 1) was carried out in which the solvent in the growth solutions (**SE2-β2-3**, **SE4-β2-2**) was predominantly acetone (97.6 % mol/ mol) in order to investigate whether the identity of the solvent would influence the mechanism of growth of the 2-D nuclei. $[Zn_4O(O_2CC_6H_5)_6]$ was crystallised from acetone so it was hypothesized that the likelihood of the $[Zn_4O(O_2CC_6H_5)_6]$ remaining intact during growth of MOF-5 was higher if acetone was used as the solvent. Results from experiment **E** are shown in Fig. 3. The experiment was performed in a similar manner to that of experiment **A**, by first introducing a **α1**-type growth solution (**SE1-α1-21**) and letting the crystal grow for approximately 2 hours. After this, solution **SE2-β2-3** was introduced that induced rapid nucleation and produced a full monolayer of MOF-5 after 5 minutes making it impossible to follow the height of developing nuclei. The nucleation rate reduced to zero after approximately 10 minutes. A second **α1**-type growth solution (**SE3-α1-17**) was introduced to promote further rapid growth in the absence of $[Zn_4O(O_2CC_6H_5)_6]$, followed by a more diluted $[Zn_4O(O_2CC_6H_5)_6]$ solution (**SE4-β2-2**). This time the nucleation rate was not as high, which allowed measurement of the development of individual nuclei on the MOF-5 surface grown from the **α1**-type growth solution. Fig. 3a shows the MOF-5 surface 5 minutes after introducing solution **SE4-β2-2**, which displays a large number of 2-D nuclei formed initially. Highlighted in the white circle is a small nuclei scanned just after formation. The accompanying cross-section shows an approximate height of 0.75 nm ± 0.1 nm, which, again, corresponds to the attachment of $bdc^{2-}$/ $Hbdc^-$ species to the MOF-5 surface. The next image (Fig. 3b) shows the nuclei now fully developed to a height of 1.2 nm ± 0.1 nm, corresponding to the standard monolayer height. Therefore, as was the case for the experiments performed in DMF, this nucleation behaviour follows that which has been reported previously for growth solutions prepared using zinc nitrate or zinc acetate salts.[19]

These results indicate that a new growth step on the surface of MOF-5 does not develop by pathway (I) in Scheme 1 in which a $bdc^{2-}$/ $Hbdc^-$ species first adds to the crystal surface followed by addition of a complete $[Zn_4O(O_2CC_6H_5)_6]$ SBU. It is hypothesised that the latter would add to the surface via a nucleophilic substitution of a benzoate group from the $[Zn_4O(O_2CC_6H_5)_6]$ molecule by a surface attached 1,4-benzenedicarboxylate unit. Such a process would make it possible to observe a step height of ~2.0 nm (see Scheme 1 pathway (I)) after addition of a $bdc^{2-}$/ $Hbdc^-$ species and a $[Zn_4O(O_2CC_6H_5)_6]$ SBU for the first terraces developing on a MOF-5 surface grown from a **α1** or **α2**-type growth solution. The result suggests that the $[Zn_4O(O_2CC_6H_5)_6]$ must undergo a degree of dissociation during the reaction to yield a species of general formula $[Zn_xO_y(O_2CC_6H_5)_z]$ (where: $x = 1 – 4$, $y = 0 – 1$, $z = 0 – 5$) prior to inclusion into a developing growth step on the surface of MOF-5 as shown in Scheme 1 pathway (II).

Incomplete dissociation, for instance leaving the complete or partial inorganic $Zn_4O$ core, may be possible that would still be likely to increase the rates of formation of MOF-5 using the SBU precursor. However, such a species was not uniquely identifiable in this study.

The results do show that, when using this SBU precursor as the source of the zinc species, the framework of MOF-5 develops through a correlated process of nucleation and spreading of different sub-layers of varying stabilities that are reliant on the presence of non-framework species for successful crystal growth.

The stoichiometry of the growth solution in terms of the Zn/ $H_2$bdc ratio was found previously to have a very important influence on the relative growth rates of MOF-5 in different crystallographic directions.[19] It was observed that with a growth solution of Zn/ $H_2$bdc ratio > 1 growth along the <100> directions was slower than along the <110> directions giving rise to square terraces. In contrast, for a growth solution of Zn/ $H_2$bdc ratio ≈ 1 growth along the <110> directions became slower, giving rise to rhombus shaped terraces with steps parallel to the <110> directions. The influence of stoichiometry of the growth solution on the growth of MOF-5 using growth solutions containing the $[Zn_4O(O_2CC_6H_5)_6]$ SBU was investigated to determine if it exhibited a similar influence as that of growth solutions prepared using zinc nitrate or zinc acetate salts. It should be noted that when quantifying the Zn/ $H_2$bdc ratio in these experiments the total number of Zn atoms was used i.e. each $[Zn_4O(O_2CC_6H_5)_6]$ molecule was considered to provide four Zn atoms. Experiment **B** was started, as in previous cases, by introducing a α1-type solution into the fluid cell to induce MOF-5 growth (solution **SB1-α1-20**). The resultant growth produced terraces with the typical square morphology, as can be seen in Fig. 4a. After a couple of hours of growth a $[Zn_4O(O_2CC_6H_5)_6]$-containing solution of Zn/ $H_2$bdc ratio ≈ 1 was injected to the fluid cell (solution **SB2-β1-1**). This solution induced 2-D nucleation which was operative for close to 3 hours, in contrast to experiment **A** (solution **SA2-β1-4**) where nucleation was confined to ~15 minutes. The measured terrace spreading rate was approximately 1.1 ± 0.1 nm $s^{-1}$, or more than two orders of magnitude higher than in experiment **SA2-β1-4**. The shape of the nuclei was fairly circular, as can be seen in Fig. 4b which shows the crystal surface 30 minutes after the solution was introduced. After a further 2.5 hours, the shape of the terraces and nuclei was still fairly circular indicating isotropic growth, as can be seen in Fig. 4c. At this point growth rates had decreased by more than 25 % and nucleation had almost stopped. Solution **SB2-β1-1** was left in the fluid cell overnight and, 21 hours after introduction, the shape of the terraces was still fairly circular (Fig. 4d) and the advancement rate had decreased by more than 80%. This indicates, that throughout the duration of the experiment growth rates along the <100> directions were similar to those along <110>. Finally, a $[Zn_4O(O_2CC_6H_5)_6]$-containing solution of Zn/ $H_2$bdc ratio ≈ 2 (solution **SB3-β1-2**) was injected into the fluid cell. This solution induced the formation of multiple 2-D nuclei (Fig. 4e) which eventually developed into square terraces (Fig. 4f).

Therefore, similarly to what has been reported on the growth of MOF-5 surface terraces from growth solutions prepared using zinc nitrate or zinc acetate salts, a growth solution with Zn/ $H_2$bdc ratio ≈ 1 (and $[Zn_4O(O_2CC_6H_5)_6]$) instigates a change in the relative growth rates in the <100> and <110> directions. However, the use of the $[Zn_4O(O_2CC_6H_5)_6]$-containing growth solutions yields a smaller change in the relative growth rates in the <100> and <110> directions compared to those grown from growth solutions prepared using zinc nitrate or zinc acetate salts.[19] This suggests that the zinc solution species derived from $[Zn_4O(O_2CC_6H_5)_6]$ is different to that derived from simpler zinc salts that might imply some degree of association of the zinc species remaining from the $[Zn_4O(O_2CC_6H_5)_6]$ cluster that influences its incorporation into the framework in growth solutions with Zn/ $H_2$bdc ratio ≈ 1.

Experiments were performed to try to determine if there was a noticeable increase in the surface nucleation and terrace spreading rates using the $[Zn_4O(O_2CC_6H_5)_6]$ SBU as the zinc precursor source. Experiments **C** and **D** were carried out where crystal growth was promoted using **α1**, **β1** and **γ1**-type growth solutions (see Table 1) with the same total Zn and $H_2$bdc concentrations. The main difference between experiments **C** and **D** was the growth solution Zn/ $H_2$bdc ratio, with experiment **C** having a ratio of ≈ 1, and experiment **D** a ratio of 8.3.

Nucleation for all three solutions in experiment **D** (**SD2-β1-8**, **SD4-α1-8**, **SD5-γ1-8**) was limited to an initial burst followed by the formation of a few nuclei which ended after less than 10 minutes. Values for the number of nuclei per unit surface area measured for the first scan taken after solution injection is given for these experiments in Table 2 in order to compare the nucleation behaviour in the three solutions. From the values given in Table 2 it is evident that the $[Zn_4O(O_2CC_6H_5)_6]$-containing solution (**SD2-β1-8**) promotes the formation of ~40 times more nuclei compared to the zinc acetate solutions (**SD4-α1-8**, **SD5-γ1-8**) indicating a strong difference in nucleation behaviour. These values support the hypothesis that the zinc solution species derived from $[Zn_4O(O_2CC_6H_5)_6]$ is different to that derived from zinc acetate and may involve some degree of association of the zinc species remaining from the $[Zn_4O(O_2CC_6H_5)_6]$ cluster that aids in promotion of surface nucleation. This would support the notion that use of a preassembled SBU enhances nucleation rates through preassembly of some component of the inorganic cluster of the subsequent MOF as is also noticeable in the rapid nucleation rates observed by Hausorf *et al.*[6] for formation of MOF-5 from SBU-containing growth solutions with a Zn/ $H_2$bdc ratio > 1. In contrast, it is the TEA-containing zinc acetate solution (**SD4-α1-8**) that results in a significantly higher terrace spreading rate with the $[Zn_4O(O_2CC_6H_5)_6]$-containing solution (**SD2-β1-8**) being the slowest. The high TEA concentration in the growth solution will deprotonate the $H_2$bdc rapidly suggesting that it is the presence of the deprotonated $Hbdc^-$/ $bdc^{2-}$ species that has a

 

greater influence on the rate of terrace spreading rather than the form or inclusion of the inorganic component.

Experiment **C** was a continuation of experiment **B**. After growing a fresh crystal surface with solution **SB3-β1-2** for approximately 1 hour, $[Zn_4O(O_2CC_6H_5)_6]$-containing solution **SC1-β1-1** was introduced. This solution produced fast, continuous nucleation which was still in operation, albeit at a much reduced rate, 130 minutes later. The nucleation rate measured over approximately 10 minutes using the first four frames taken after solution introduction for this solution was 0.09 ± 0.02 nuclei $s^{-1}$ $\mu m^{-2}$ (see Table 2). Solution **SC2-γ1-1** (zinc acetate with no TEA) produced a similar effect although with a much higher nucleation rate (0.20 ± 0.04 nuclei $s^{-1}$ $\mu m^{-2}$). Finally solution **SC3-α1-1** (zinc acetate with TEA) resulted also in continuous nucleation with a rate very similar to that of solution **SC1-β1-1** (0.08 ± 0.02 nuclei $s^{-1}$ $\mu m^{-2}$). These results indicate that solutions containing zinc acetate in the absence of TEA (**SC2-γ1-1**) results in the greatest nucleation rate. This suggests that the nucleation process occurs through a different mechanism for growth solutions with a Zn/ $H_2$bdc ratio of ≈ 1 that is less dependent on the form of the zinc solution species. The measured terrace spreading rates for the three experiments are shown in Table 2. Again, it can be seen that the fastest terrace spreading rate was produced for the TEA-containing solution (**SC3-α1-1**). This again supports the idea that it is the presence of the deprotonated $Hbdc^-$/ $bdc^{2-}$ species that has the greatest influence on the rate of terrace spreading than the form or inclusion of the inorganic component.

One final trend that is noticeable from the data provided in Table 2 is that similar or higher nucleation and higher terrace spreading rates are observed for comparable experiments with $[Zn_4O(O_2CC_6H_5)_6]$-containing solutions (**SA2-β1-4** v **SD2-β1-8**, **SB2-β1-1** v **SC1-β1-1**) with a higher $H_2$bdc concentration. The results also indicate that the $H_2$bdc concentration has more influence on these rates than the zinc species concentration for the growth solutions of Zn/ $H_2$bdc ratio > 1 (**SA2-β1-4** v **SD2-β1-8**). This trend may be a reflection of the fact that the first process involved in nucleation and terrace spreading is the attachment of $Hbdc^-$/ $bdc^{2-}$ to zinc species in the terminating crystal surface.

More definitive conclusions concerning the influence of the various components upon the rates of these processes is currently not possible owing to the complexity of the system, and the lack of information regarding the solution speciation in MOF-5 syntheses.

## Conclusions

The crystal growth of MOF-5 involving a zinc-containing SBU has been observed in real time for the first time through use of *in situ* AFM. 2-D nuclei were found to form by a two-step process whereby $Hbdc^-$/ $bdc^{2-}$ units first attach to the MOF-5 surface, followed by the completion of the monolayer by addition of Zn species and linking $bdc^{2-}$ units. No evidence of a growth mechanism involving nucleophilic substitution of benzoate groups from intact $[Zn_4O(O_2CC_6H_5)_6]$ molecules by surface attached 1,4-benzenedicarboxylate units was found. This indicates that the $[Zn_4O(O_2CC_6H_5)_6]$ molecules undergo a degree of dissociation before incorporation into the MOF-5 framework. The SBU-containing growth solutions were found to influence the relative growth rates along different crystallographic directions and to lead to a faster nucleation rate under certain conditions when compared to growth solutions containing simpler zinc salts. This suggests a degree of remnant association of the zinc species derived from the SBU cluster during crystal growth under these low superaturation conditions. These results suggest that the crystal growth of MOFs involving SBUs at low supersaturation may not occur by a simple connection of the complete SBUs via ligand substitution reactions but is likely to proceed by a significantly more complex mechanism that remains to be fully elucidated. The work also suggests that the advantages of MOF synthesis using preformed SBUs may be attained using simpler partially associated inorganic species rather than a full SBU which could potentially increase the range and simplicity of the starting inorganic species used in the formation of MOFs via a SBU-type approach.

## Acknowledgements

The authors wish to acknowledge the Leverhulme Trust and the EPSRC for funding, and the Nuffield Foundation for provision of a Chemistry Undergraduate Research Bursary for KE.

## Notes and references

[a] *Centre for Nanoporous Materials. School of Chemistry. The University of Manchester. Oxford Rd. M13 9PL. Manchester, UK. Fax: +44-161-275-4598; Tel: +44-161-306-4467; E-mail: m.attfield@manchester.ac.uk*
[#] *Current address: Department of Earth Sciences, Durham University, DH1 3LE, Durham, UK.*

Electronic Supplementary Information (ESI) available: PXRD pattern and SEM image of MOF-5 substrate material and PXRD pattern of $[Zn_4O(O_2CC_6H_5)_6]$ precursor. See DOI: 10.1039/b000000x/

1. H. C. Zhou, J. R. Long and O. M. Yaghi, *Chem. Rev.*, 2012, **112**, 673.
2. G. Ferey, *Chem. Soc. Rev.*, 2008, **37**, 191.
3. J. L. C. Rowsell and O. M. Yaghi, *Micropor. Mesopor. Mater.*, 2004, **73**, 3.
4. S. Bureekaew, S. Shimomura and S. Kitagawa, *Sci. Technol. Adv. Mater.*, 2008, **9**, 014108.
5. C. Serre, F. Millange, S. Surblé and G. Férey, *Angew. Chem., Int. Ed.*, 2004, **43**, 6285.
6. S. Hausdorf, F. Baitalow, T. Bohle, D. Rafaja and F. O. R. L. Mertens, *J. Am. Chem. Soc.*, 2010, **132**, 10978.
7. V. Guillerm, S. Gross, C. Serre, T. Devic, M. Bauer and G. Ferey, *Chem. Commun.*, 2010, **46**, 767.
8. R. Nayuk, D. Zacher, R. Schweins, C. Wiktor, R. A. Fischer, G. van Tendeloo and K. Huber, *J. Phys. Chem. C*, 2012, **116**, 6127.
9. A. S. Munch, M. S. Lohse, S. Hausdorf, G. Schreiber, D. Zacher, R. A. Fischer and F. O. R. L. Mertens, *Micropor. Mesopor. Mater.*, 2012, **159**, 132.

10. S. Surble, F. Millange, C. Serre, G. Ferey and R. I. Walton, *Chem. Commun.*, 2006, 1518.
11. A. McPherson, Y. G. Kuznetsov, A. Malkin and M. Plomp, *J. Struct. Biol.*, 2003, **142**, 32.
12. H. H. Teng, P. M. Dove and J. J. De Yoreo, *Geochim. Cosmochim. Acta*, 2000, **64**, 2255.
13. S. R. Higgins and X. M. Hu, *Geochim. Cosmochim. Acta*, 2005, **69**, 2085.
14. R. Brent, P. Cubillas, S. M. Stevens, K. E. Jelfs, A. Umemura, J. T. Gebbie, B. Slater, O. Terasaki, M. A. Holden and M. W. Anderson, *J. Am. Chem. Soc.*, 2010, **132**, 13858.
15. M. Shoaee, M. W. Anderson and M. P. Attfield, *Angew. Chem., Int. Ed.*, 2008, **47**, 8525.
16. N. S. John, C. Scherb, M. Shoaee, M. W. Anderson, M. P. Attfield and T. Bein, *Chem. Commun.*, 2009, 6294.
17. P. Y. Moh, P. Cubillas, M. W. Anderson and M. P. Attfield, *J. Am. Chem. Soc.*, 2011, **133**, 13304.
18. P. Cubillas, M. W. Anderson and M. P. Attfield, *Cryst. Growth Des.*, 2013, **13**, 4526.
19. P. Cubillas, M. W. Anderson and M. P. Attfield, *Chem. Eur. J.*, 2012, **18**, 15406.
20. H. Li, M. Eddaoudi, M. O'Keeffe and O. M. Yaghi, *Nature*, 1999, **402**, 276.
21. J. L. C. Rowsell, E. C. Spencer, J. Eckert, J. A. K. Howard and O. M. Yaghi, *Science*, 2005, **309**, 1350.
22. G. Blustein, R. Romagnoli, J. A. Jaen, A. R. Di Sarli and B. del Amo, *Colloid Surf. A-Physicochem. Eng. Asp.*, 2006, **290**, 7.
23. W. Clegg, D. R. Harbron, C. D. Homan, P. A. Hunt, I. R. Little and B. P. Straughan, *Inorganica Chimica Acta*, 1991, **186**, 51.
24. D. J. Tranchemontagne, J. R. Hunt and O. M. Yaghi, *Tetrahedron*, 2008, **64**, 8553.

**Fig. 1.** The structure of MOF-5 viewed along the [001] direction. The structure is shown in stick and polyhedral modes: blue tetrahedra = Zn-centred $ZnO_4$ tetrahedra, red sticks = bdc linkers, H omitted for clarity.

**Fig. 2.** (a and b) AFM deflection images taken ca. 2 minutes apart during experiment **SA2-β1-4** showing the development of the 2-D nuclei centred in the white circle. Cross-sectional analyses and structural diagrams of the equivalent height in the MOF-5 crystal structure are also displayed for each image. Scale bars for (a) and (b) are identical. The structure is shown in ball and stick mode: blue = Zn, red = O, black = C, H omitted for clarity.

**Fig. 3.** (a and b) AFM deflection images taken ca. 2 minutes apart during experiment **SE4-β2-2** showing the development of the 2-D nuclei centred in the white circle. Cross-sectional analysis is also displayed for each image. Scale bars for (a) and (b) are identical.

**Fig. 4.** AFM deflection images of a {100} face captured at certain times during experiment **B** showing the formation of (a) square terraces of MOF-5 in solution **SB1-α1-20** with Zn/ $H_2$bdc ratio > 1, (b - d) rounded terraces of MOF-5 in solution **SB2-β1-1** with Zn/ $H_2$bdc ratio ≈ 1 taken after progressively longer times after the introduction of solution **SB2-β1-1**, (e - f) square terraces of MOF-5 in solution **SB3-β1-2** with Zn/ $H_2$bdc ratio >1 taken after progressively longer times after the introduction of solution **SB3-β1-2**.

**Scheme 1.** Possible pathways to the formation of a new monolayer on the surface of MOF-5 involving the $[Zn_4O(O_2CC_6H_5)_6]$ SBU and $H_2$bdc/ $Hbdc^-$/ $bdc^{2-}$. The structures are shown in polyhedral and ball and stick mode: blue tetrahedra = Zn, red balls = O, black balls = C, H omitted for clarity.

## Table of Contents

Growth studies of MOF-5 using $[Zn_4O(O_2CC_6H_5)_6]$ SBUs reveal that the SBUs do not remain intact but their form does influence the relative rates of certain growth processes.

**Table 1.** Summary of the chemical composition and Zn/ $H_2$bdc ratios for all the growth solutions.

| Experiment | Solution* | $Zn(OAc)_2 \cdot 2H_2O$ [mol] | $[Zn_4O(O_2CC_6H_5)_6]$ [mol] | $H_2$bdc [mol] | TEA [mol] | DMF [mol] | Acetone [mol] | Zn [mol] | Zn/$H_2$bdc |
|---|---|---|---|---|---|---|---|---|---|
| **A** | **SA1-α1-21** | 0.0248 | - | 0.0012 | 0.0682 | 11.62 | - | 0.0248 | 21.3 |
| | **SA2-β1-4** | - | 0.00150 | 0.0015 | - | 11.62 | - | 0.0060 | 4.0 |
| **B** | **SB1-α1-20** | 0.0225 | - | 0.0011 | 0.0682 | 11.62 | - | 0.0225 | 20.3 |
| | **SB2-β1-1** | - | 0.00074 | 0.0030 | - | 11.62 | - | 0.0030 | 1.0 |
| | **SB3-β1-2** | - | 0.00099 | 0.0020 | - | 11.62 | - | 0.0039 | 2.0 |
| **C** | **SC1-β1-1** | - | 0.00056 | 0.0023 | - | 11.62 | - | 0.0023 | 1.0 |
| | **SC2-γ1-1** | 0.0023 | - | 0.0023 | - | 11.62 | - | 0.0023 | 1.0 |
| | **SC3-α1-1** | 0.0023 | - | 0.0023 | 0.0682 | 11.62 | - | 0.0023 | 1.0 |
| **D** | **SD1-α1-19#** | 0.0205 | - | 0.0011 | 0.0682 | 11.62 | - | 0.0205 | 18.9 |
| | **SD2-β1-8** | - | 0.00224 | 0.0011 | - | 11.62 | - | 0.0090 | 8.3 |
| | **SD3-α1-19#** | 0.0205 | - | 0.0011 | 0.0682 | 11.62 | - | 0.0205 | 18.9 |
| | **SD4-α1-8** | 0.0090 | - | 0.0011 | 0.0682 | 11.62 | - | 0.0090 | 8.3 |
| | **SD5-γ1-8** | 0.0090 | - | 0.0011 | - | 11.62 | - | 0.0090 | 8.3 |
| **E** | **SE1-α1-21** | 0.0225 | - | 0.0011 | 0.0682 | 11.62 | - | 0.0225 | 20.8 |
| | **SE2-β2-3** | - | 0.00065 | 0.0011 | - | 0.29 | 11.62 | 0.0026 | 2.5 |
| | **SE3-α1-17** | 0.0184 | - | 0.0011 | 0.0682 | 11.62 | - | 0.0184 | 17.0 |
| | **SE4-β2-2** | - | 0.00035 | 0.0009 | - | 0.29 | 11.62 | 0.0014 | 1.5 |

*Solution naming scheme **SVW-XY-Z**: where **S -** solution, **V -** experiment (**A - E**), **W** - the order the growth solution was used within an experiment, with **1** being the first growth solution injected, **X -** solution type in terms of zinc source and presence or absence of TEA (**α -** $Zn(OAc)_2 \cdot 2H_2O$ and TEA, **β** - $[Zn_4O(O_2CC_6H_5)_6]$, **γ** - $Zn(OAc)_2 \cdot 2H_2O$), **Y** – solvent (**1** - DMF, **2** - DMF/ Acetone), **Z –** initial Zn/ $H_2$bdc ratio growth solution.

#Growth solution not mentioned in results but included for completeness of experimental procedure.

**Table 2.** The terrace spreading rates, nucleation rates and number of nuclei formed per area measured for some of the experiments listed in Table 1

| Experiment | Solution[1] | Growth rate[2] (nm $s^{-1}$) | Nucleation rate[3] (nuc $s^{-1}$ $\mu m^{-2}$) | Nuclei per area[3](nuc $\mu m^{-2}$) |
|---|---|---|---|---|
| **A** | **SA2-β1-4** | 0.02 | - | 8.7 |
| **B** | **SB2-β1-1** | 1.05 | 0.06 ± 0.005 | - |
| **C** | **SC1-β1-1** | 0.66 | 0.09 ± 0.011 | - |
| | **SC2-γ1-1** | 0.43 | 0.20 ± 0.014 | - |
| | **SC3-α1-1** | 1.32 | 0.08 +0.005 | - |
| **D** | **SD2-β1-8** | 0.01 | - | 3.7 |
| | **SD4-α1-8** | 0.46 | - | 0.1 |
| | **SD5-γ1-8** | 0.41 | - | 0.08 |

[1.] See Table 1 footnote for solution naming scheme.

[2.] Measurement has an approximate 10 - 25 % standard deviation.

[3.] A 25% standard deviation is assumed on these measurements.

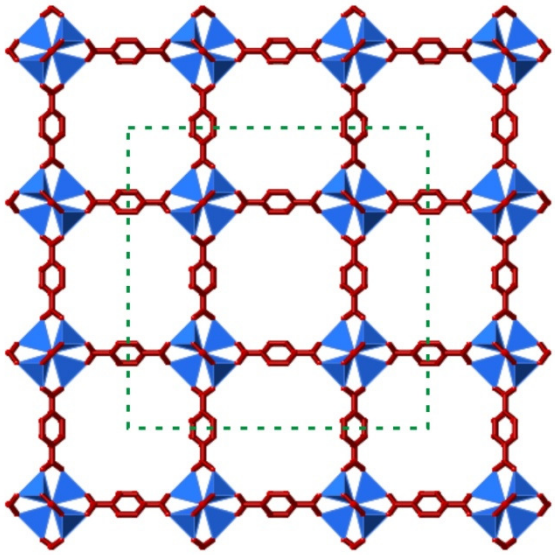

**Fig. 1.** The structure of MOF-5 viewed along the [001] direction. The structure is shown in stick and polyhedral modes: blue tetrahedra = Zn-centred $ZnO_4$ tetrahedra, red sticks = bdc linkers, H omitted for clarity.

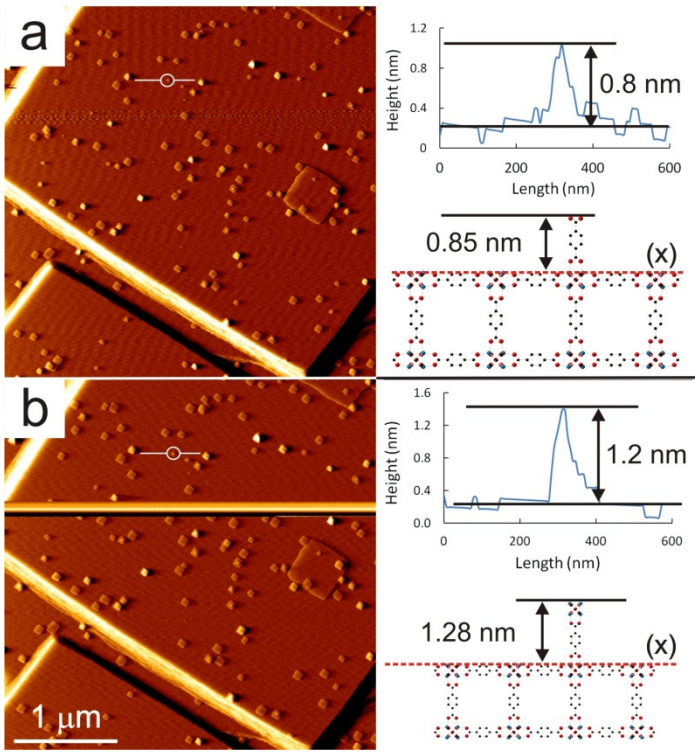


**Fig. 2.** (a and b) AFM deflection images taken ca. 2 minutes apart during experiment **SA2-β1-4** showing the development of the 2-D nuclei centred in the white circle. Cross-sectional analyses and structural diagrams of the equivalent height in the MOF-5 crystal structure are also displayed for each image. Scale bars for (a) and (b) are identical. The structure is shown in ball and stick mode: blue = Zn, red = O, black = C, H omitted for clarity.

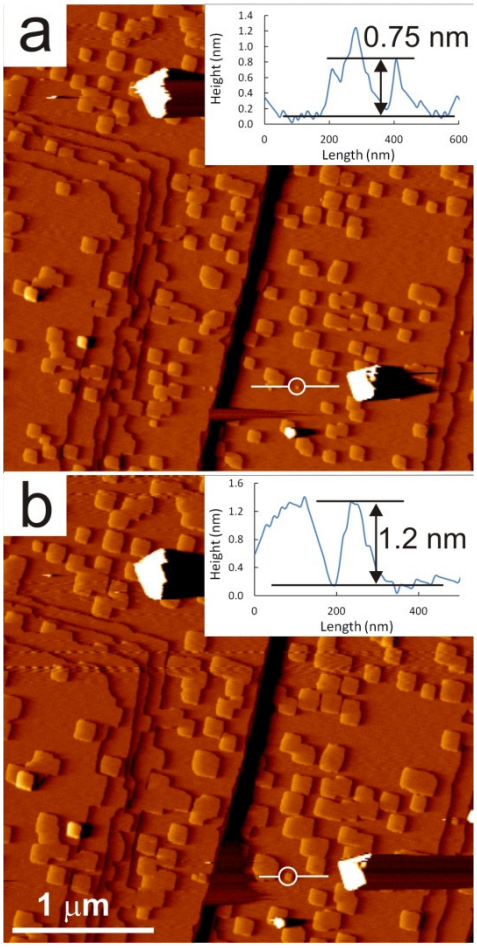


**Fig. 3.** (a and b) AFM deflection images taken ca. 2 minutes apart during experiment **SE4-β2-2** showing the development of the 2-D nuclei centred in the white circle. Cross-sectional analysis is also displayed for each image. Scale bars for (a) and (b) are identical.

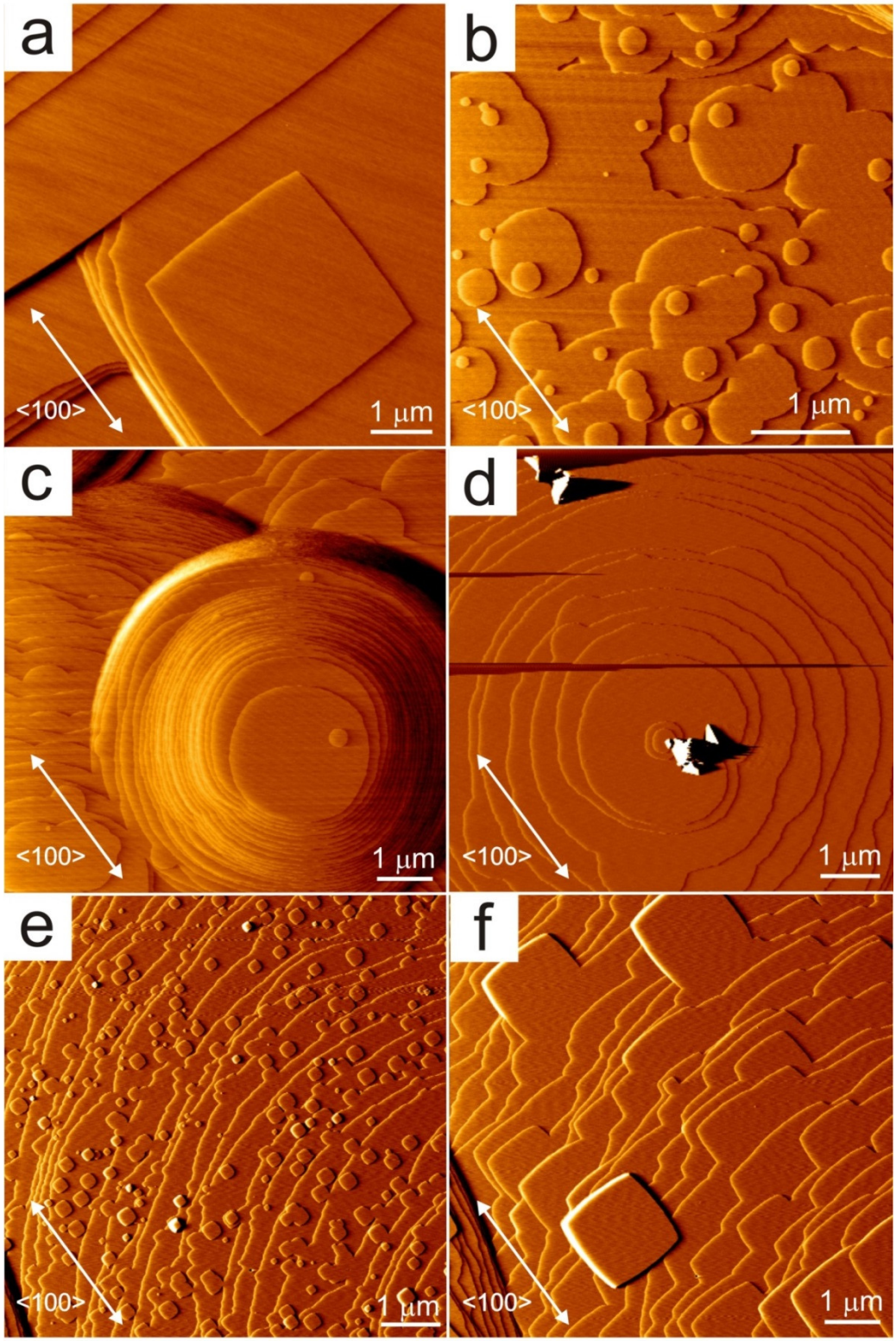


**Fig. 4.** AFM deflection images of a {100} face captured at certain times during experiment **B** showing the formation of (a) square terraces of MOF-5 in solution **SB1-α1-20** with Zn/ $H_2$bdc ratio > 1, (b - d) rounded terraces of MOF-5 in solution **SB2-β1-1** with Zn/ $H_2$bdc ratio ≈ 1 taken after progressively longer times after the introduction of solution **SB2-β1-1**, (e - f) square terraces of MOF-5 in solution **SB3-β1-2** with Zn/ $H_2$bdc ratio >1 taken after progressively longer times after the introduction of solution **SB3-β1-2**.

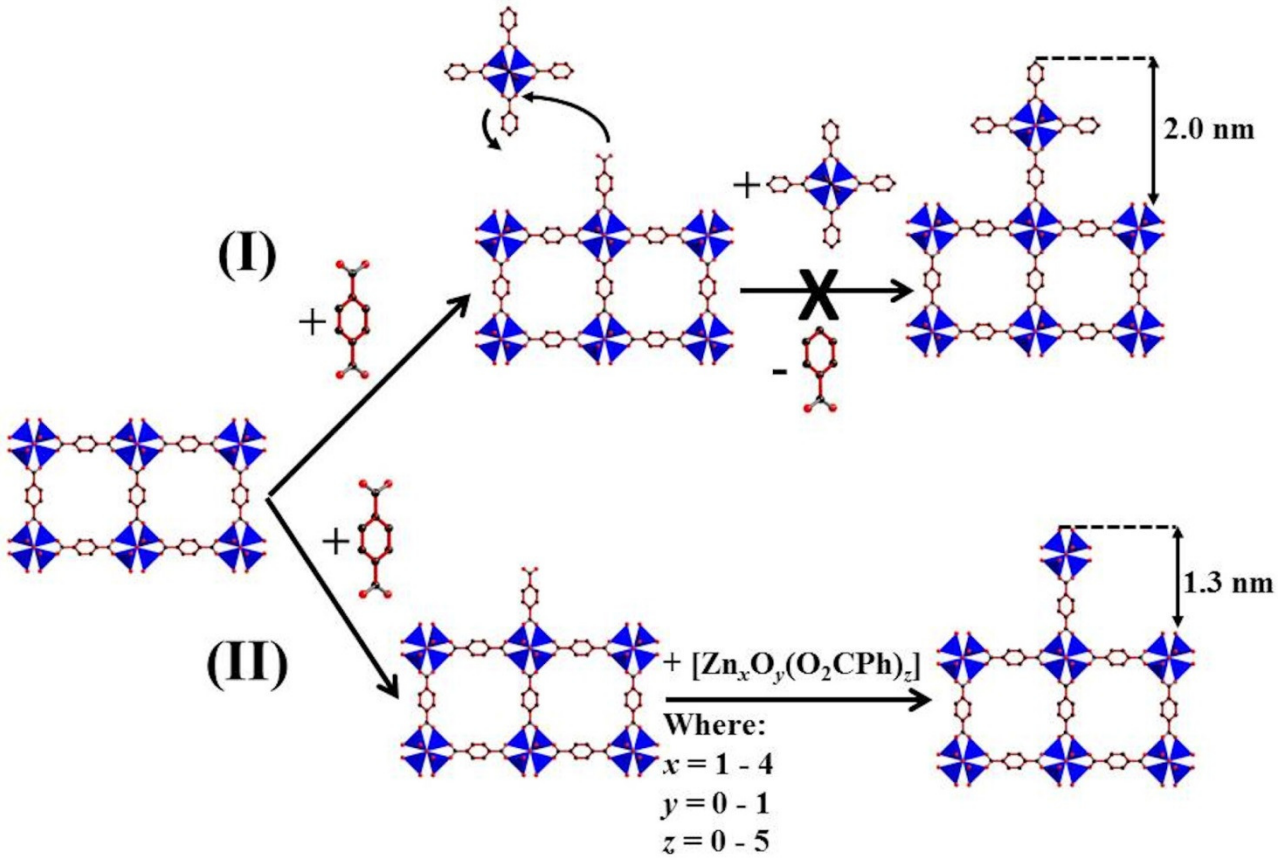


**Scheme 1.** Possible pathways to the formation of a new monolayer on the surface of MOF-5 involving the $[Zn_4O(O_2CC_6H_5)_6]$ SBU and $H_2bdc$/ $Hbdc^-$/ $bdc^{2-}$. The structures are shown in polyhedral and ball and stick mode: blue tetrahedra = Zn, red balls = O, black balls = C, H omitted for clarity.

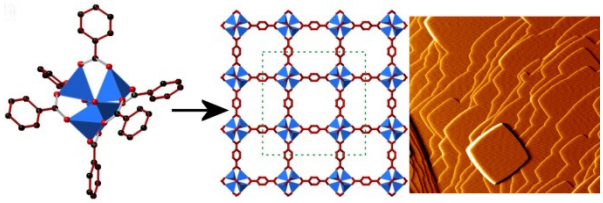

**Graphical Abstract**